REAL TIME IMPLEMENTATION OF MRAS AND DESIGN KALMAN FILTER BASED SPEED SENSORLESS VECTOR CONTROL OF INDUCTION MOTOR

K. NEGADI A. MANSOURI
Physics Engineering Laboratory, Ibn khaldoun University of Tiaret,
BP 78- Tiaret, Algeria, e-mail: negadi_k@yahoo.fr
Laboratory of Automatics and Systems Analysis (L.A.A.S.), Department of Electrical Engineering, E.N.S.E.T. Oran BP 1523 El' M'naouer, Oran, Algeria, e-mail: ammansouri@yahoo.fr

B. KHATEMI
Faculty of Science and Engineering, Ibn khaldoun University of Tiaret,
BP 78 Tiaret, Algeria, e-mail: khatemi.belkheir@yahoo.fr

Abstract: *Sensorless induction motor drives are widely used in industry for their reliability and flexibility. However, rotor flux and speed sensors are required for vector control of induction motor. These sensors are sources of trouble, mainly in hostile environments, and their application reduces the drive robustness. The cost of the sensors is not also negligible. All the reasons lead to development of different sensorless methods for rotor flux and mechanical speed estimation in electrical drives. The paper deals with the speed estimators for applications in sensorless induction motor drive with vector control, which are based on application of model adaptive based Kalman filter methods. The development and DSP implementation of the speed estimators for applications in sensorless drives with induction motor are described in the paper.*

Key words: *Sensorless control, induction motor drives, Kalman filter estimator, MRAS, modeling, field oriented control, Dspace.*

1. Introduction

Induction motor drives have been thoroughly studied in the past few decades and many vector control strategies have been proposed, ranging from low cost to high performance applications. In order to increase the reliability and reduce the cost of the drive, a great effort has been made to eliminate the shaft speed sensor in most high performance induction motor drive applications [1]. Speed estimation is an issue of particular interest with induction motor drives where the mechanical speed of the rotor is generally different from the speed of the revolving magnetic field. The advantages of speed sensorless induction motor drives are reduced hardware complexity and lower cost, reduced size of the drive motor, better immunity, elimination of the sensor cable, increased reliability and less maintenance requirements. The induction motor is however relatively difficult to control compared to other types of electrical motors. For high performance control, field oriented control is the most widely used control strategy. This strategy requires information of the flux in motor; however the voltage and current model observers are normally used to obtain this information. Generally, using the induction motor state equations, the flux and speed can be calculated from the stator voltage and current values. This paper presents model adaptive Kalman estimators for the proposed control.

2. Motor model and vector control strategy

The induction motor mathematical model in d-q coordinates established in a rotor flux oriented reference frame can be written as [2]:

$$v_{sd} = R_s i_{sd} + \frac{d\Psi_{sd}}{dt} - \omega_e \Psi_{sq} \quad (1)$$

$$v_{sq} = R_s i_{sq} + \frac{d\Psi_{sq}}{dt} + \omega_e \Psi_{sd} \quad (2)$$

$$0 = R_r i_{rd} + \frac{d\Psi_{rd}}{dt} - \omega_{sl} \Psi_{rq} \quad (3)$$

$$0 = R_r i_{rq} + \frac{d\Psi_{rq}}{dt} + \omega_{sl} \Psi_{rd} \quad (4)$$

where the stator and rotor flux linkages are given by:

$$\Psi_{sd} = L_s i_{sd} + L_m i_{rd} \quad (5)$$

$$\Psi_{sq} = L_s i_{sq} + L_m i_{rq} \quad (6)$$

$$\Psi_{rd} = L_r i_{rd} + L_m i_{sd} \quad (7)$$

$$\Psi_{rq} = L_r i_{rq} + L_m i_{sq} \quad (8)$$

The state space representation of the induction motor with the stator currents and the rotor flux linkages components as state variables can be written as:

$$\begin{bmatrix} \frac{d}{dt}i_{sd} \\ \frac{d}{dt}i_{sq} \\ \frac{d}{dt}\Psi_{rd} \\ \frac{d}{dt}\Psi_{rq} \end{bmatrix} = \begin{bmatrix} -\left(\frac{R_s}{\sigma L_s}+\frac{1-\sigma}{\sigma T_r}\right) & \omega_e & \frac{L_m}{\sigma L_s L_r T_r} & \left(\frac{L_m}{\sigma L_s L_r}\right)\omega_r \\ -\omega_e & -\left(\frac{R_s}{\sigma L_s}+\frac{1-\sigma}{\sigma T_r}\right) & -\left(\frac{L_m}{\sigma L_s L_r}\right)\omega_r & \frac{L_m}{\sigma L_s L_r T_r} \\ \frac{L_m}{T_r} & 0 & \frac{-1}{T_r} & (\omega_e-\omega_r) \\ 0 & \frac{L_m}{T_r} & -(\omega_e-\omega_r) & \frac{-1}{T_r} \end{bmatrix} \begin{bmatrix} i_{sd} \\ i_{sq} \\ \Psi_{rd} \\ \Psi_{rq} \end{bmatrix} + \begin{bmatrix} \frac{1}{\sigma L_s} & 0 \\ 0 & \frac{1}{\sigma L_s} \\ 0 & 0 \\ 0 & 0 \end{bmatrix} \begin{bmatrix} v_{sd} \\ v_{sq} \end{bmatrix} \tag{9}$$

where T_r is the rotor time constant and is given by:

$$T_r = \frac{R_r}{L_r}$$

and σ is the leakage coefficient given by:

$$\sigma = 1 - \frac{L_m^2}{L_r L_s}$$

The electromagnetic torque and the rotor speed are given by:

$$T_{em} = \frac{3}{2} p \frac{L_m}{JL_r} (\Psi_{rd} i_{sq} - \Psi_{rq} i_{sd}) \tag{10}$$

where:

R_s and R_r are the stator and rotor winding resistances; L_s, L_m and L_r are the stator, mutual and rotor inductances; p is the number of pole pairs; ω_e, ω_r and ω_{sl} are the synchronous, rotor and slip speed in electrical rad/s; v_{sd}, v_{sq}, i_{sd}, i_{sq}, Ψ_{rd} and Ψ_{rq} are stator voltage, stator current and rotor flux d-q components in the rotor flux oriented reference frame; T_{em} and T_l are the electromagnetic torque and the load torque respectively; J and f are the motor inertia and viscous friction coefficient respectively Under the rotor flux orientation conditions the rotor flux is aligned on the d-axis of the d-q rotor flux oriented frame and the rotor flux equations can be written as:

$$\Psi_{rq} = 0 \tag{11}$$

$$\Psi_{rd} = L_m i_{sd} \tag{12}$$

The electromagnetic torque equation can be written as:

$$T_{em} = \frac{3}{2} p \frac{L_m}{L_r} \Psi_r i_{sq} = K_t i_{sq} \tag{13}$$

where K_t is the torque constant given by:

$$K_t = \frac{3}{2} p \frac{L_m}{L_r} \Psi_r \tag{14}$$

3. Model Reference Adaptive Systems (MRAS)

The basic concept of MRAS is the presence of a reference model which determines the desired states and an adaptive (adjustable) model which generates the estimated values of the states. The error between these states is fed to an adaptation mechanism to generate an estimated value of the rotor speed which is used to adjust the adaptive model. This process continues till the error between two outputs tends to zero [3, 4]. Basic equations of rotor flux based-MRAS can be written as:

$$\Psi_r = \left(\frac{L_r}{L_m}\right)\left[\int (v_s - R_s i_s)dt - L_s i_s\right] \tag{15}$$

$$\hat{\Psi}_r = \left(\frac{1}{T_r}\right)\int (L_m i_s - \hat{\Psi}_r - \hat{\omega} T_r \hat{\Psi}_r)dt \tag{16}$$

The reference model (15) is based on stator equations and is therefore independent of the motor speed, while the adaptive model (16) is speed-dependant since it is derived from the rotor equation in the stationary reference frame. To obtain a stable nonlinear feedback system, a speed tuning signal (ε_ω) and a PI controller [5] are used in the adaptation mechanism to generate the estimated speed. The speed tuning signal and the estimated speed expressions can be written as:

$$\varepsilon_\omega = \Psi_{rq} \hat{\Psi}_{rd} - \Psi_{rd} \hat{\Psi}_{rq} \tag{17}$$

$$\hat{\omega} = \left\{K_p + \frac{K_i}{s}\right\}\varepsilon_\omega \tag{18}$$

where: K_p, K_i are the proportional and integral constants.

Generally the MRAS observer gives satisfactory speed estimation in the high and medium speed regions. When working at low speed the observer performance deteriorates due to integrator drift and initial condition problems and sensitivity to current measurement noise. Therefore a Kalman filter estimator is proposed to replace the conventional adaptive model (16), (fig. 1) to improve the MRAS scheme performance at load condition, reversal speed and low speed region [6].

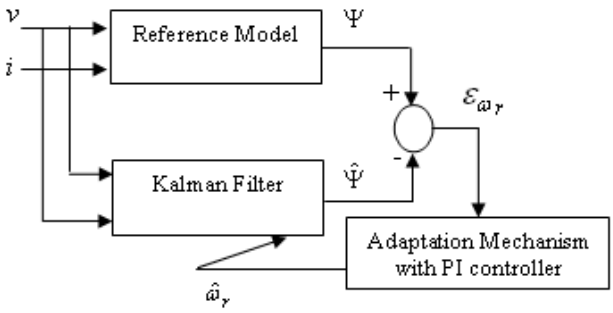

Fig. 1. Kalman filter with MARS observer.

4. Presentation of Kalman Filter Algorithm

The Kalman filter algorithm is robust and efficient observer for linear and nonlinear systems, as it is the case of induction motor. The KF use knowledge about the system dynamics and statistical properties of the system, and measurement noise sources to produce an optimal state estimation. The application of the KF algorithm consists on two phases [7]:

Prediction phase

$$\hat{x}_{k+1/k} = A_{k/k}.\hat{x}_{k/k} + B_{k/k}.u_k \quad (19)$$

$$p_{k+1/k} = A_{k/k}.p_{k/k}.A_{k/k}^{T} + Q_k \quad (20)$$

$\hat{x}_k$ is the state estimate, P_k is the estimate error covariance matrix and Q_k covariance matrix of the system noise.

Correction phase

At the instant $(k+1)$, the predicted state variables and their covariance are corrected by using:

$$K_{k+1} = p_{k+1/k}.C_k^T\left(C_k.p_{k+1/k}.C_k^T + R_k\right)^{-1} \quad (21)$$

$$p_{k+1/k+1} = \left(I - K_{k+1}.C_k\right).p_{k+1/k} \quad (22)$$

$$\hat{x}_{k+1/k+1} = \hat{x}_{k+1/k} + K_{k+1}.\left(y_{k+1} - C_k.\hat{x}_{k+1/k}\right) \quad (23)$$

K is the Kalman gain matrix.

5. Design of kalman filter for induction motor

For the implementation of the algorithm of Kalman filter, the model of the induction motor given by (9) must be discrete. The discrete model of the motor is given by the equation bellow [8]:

$$x_{k+1/k} = f(A_{k/k}.x_{k/k} + B_{k/k}.u_k) \quad (24)$$

$$y_k = C_k x_k \quad (25)$$

If the system matrix, the input and output matrices of the discrete system are denoted by A_k, B_k and C_k, while the state and the output of the discrete system are denoted by x_k and y_k, then, we defined the function:

$$F = f(A_k x_k + B_k u_k) \quad (26)$$

$$H = C_k x_k \quad (27)$$

$$F = \begin{bmatrix} 1 - T_e\left(\frac{R_s}{\sigma L_s} + \frac{1-\sigma}{\sigma T_r}\right) + T_e\omega_e + \frac{T_e L_m}{\sigma L_s L_r T_r} + T_e\left(\frac{L_m}{\sigma L_s L_r}\right)\omega_r + \frac{T_e v_{sd}}{\sigma L_s} \\ -T_e\omega_e + \left(1 - T_e\left(\frac{R_s}{\sigma L_s} + \frac{1-\sigma}{\sigma T_r}\right)\right) - T_e\left(\frac{L_m}{\sigma L_s L_r}\right)\omega_r + \frac{T_e L_m}{\sigma L_s L_r T_r} + \frac{T_e v_{sq}}{\sigma L_s} \\ \frac{T_e L_m}{T_r} + 1 + \frac{T_e}{T_r} + T_e(\omega_e - \omega_r) \\ \frac{T_e L_m}{T_r} - T_e(\omega_e - \omega_r) + 1 + \frac{T_e}{T_r} \end{bmatrix}$$

$$H = \begin{bmatrix} 1 & 0 & 0 & 0 \\ 0 & 1 & 0 & 0 \end{bmatrix}$$

where T_e is the sampling time

From (26) and (27), the matrices F, H, $\frac{\partial F}{\partial x}$, $\frac{\partial H}{\partial x}$ are obtained as follows [9]:

$$\frac{\partial F}{\partial x} = \begin{bmatrix} 1 - T_e\left(\frac{R_s}{\sigma L_s} + \frac{1-\sigma}{\sigma T_r}\right) & T_e\omega_e & \frac{T_e L_m}{\sigma L_s L_r T_r} & T_e\left(\frac{L_m}{\sigma L_s L_r}\right)\omega_r \\ -T_e\omega_e & 1 - T_e\left(\frac{R_s}{\sigma L_s} + \frac{1-\sigma}{\sigma T_r}\right) & -T_e\left(\frac{L_m}{\sigma L_s L_r}\right)\omega_r & \frac{T_e L_m}{\sigma L_s L_r T_r} \\ \frac{T_e L_m}{T_r} & 0 & 1 + \frac{T_e}{T_r} & T_e(\omega_e - \omega_r) \\ 0 & \frac{T_e L_m}{T_r} & -T_e(\omega_e - \omega_r) & 1 + \frac{T_e}{T_r} \end{bmatrix} \quad (28)$$

$$\frac{\partial H}{\partial x} = \begin{bmatrix} 1 & 0 & 0 & 0 \\ 0 & 1 & 0 & 0 \end{bmatrix} \quad (29)$$

The implementation of algorithm of the Kalman filter is very easy using the Embedded Matlab function block is based on an M-file written in the MATLAB language because it can be supported by RTI (Reat Time Interface). We use only the estimated d-q axis flux with the reference model of MRAS to calculate the rotor speed using a PI controller, the convergence of the algorithm is assured with simple time Te=10^{-4}, use Euler method and the choices of the error covariance matrix P of the Kalman filter is initially set as a unit matrix and the measurement noise covariance matrix R and Q can not be calculated, they must be filled based on experimental investigations. In the following experiments, the best filter performance was obtained with:

$$P = \begin{bmatrix} 1 & 0 & 0 & 0 \\ 0 & 1 & 0 & 0 \\ 0 & 0 & 1 & 0 \\ 0 & 0 & 0 & 1 \end{bmatrix},\ R = \begin{bmatrix} 0.001 & 0 \\ 0 & 0.001 \end{bmatrix},$$

$$Q = \begin{bmatrix} 10^{-2} & 0 & 0 & 0 \\ 0 & 10^{-2} & 0 & 0 \\ 0 & 0 & 10^{-1} & 0 \\ 0 & 0 & 0 & 10^{-2} \end{bmatrix}$$

6. Description of Laboratory Setup

The adaptive Kalman filter speed observer has been tested experimentally on a suitable test setup (fig .2). The test setup consists of the following:

- Three-phase induction motor with rated values shown in Table I;
- Synchronous machine for loading the induction motor;
- Electronic power converter: three-phase diode rectifier and VSI composed of three IGBT modules without any control system;
- Electronic card with voltage sensors (model LEM LV 25-P) and current sensors (model LEM LA 55-P) for monitoring the instantaneous values of the stator phase voltages and currents;
- Voltage sensor (model LEM CV3-1000) for monitoring the instantaneous value of the dc-link

voltage;
• Incremental encoder (model RS 256-499, 2500 pulses per round), only for comparison measurements;
• dSPACE card (model DS1104) with a PowerPC 604e at 400 MHz and a floating-point digital signal processor (DSP) TMS320F240.

During the real-time operation of the control algorithm, the supervision and capturing of the important data can be done by the CONTROLDESK software provided with the DSP board. Experimental results are captured on the CONTROLDESK and imported to workspace through structure DATA file.

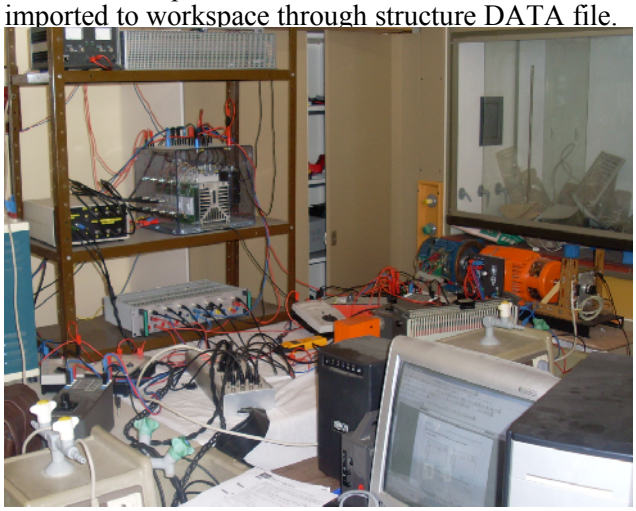

Fig. 2. Experimental setup.

7. Experimental Results and Discussion

The adaptive Kalman filter has been verified experimentally to the test bench described in Section 6. Simulations have been performed in the Matlab-Simulink environment. With regard to the experimental tests the speed observers as well as the whole control algorithm have been implemented by software on the the dSPACE board by employing the Matlab-Simulink Real Time Workshop- Real Time Interface environment. Flux reference is set to its rated value and the dc link voltage is 500 V. Some experimental results were provided to demonstrate the effectiveness of the proposed observer technique. First experiment, the target speed is changed from 0 rpm to 1490 rpm at 1.5 sec with no load applied Fig 3 shows the experimental result of a speed at free acceleration using the estimation of speed, rotor flux and flux angle to control the motor. Additionally, the real speed is measured and compared. It can be seen that there is a very good accordance between real and estimated speed without any steady state error. Fig 4 depicts the trajectories of the electromagnetic torque (a), estimated and measured stator currents evolution (b). It should be noted that the amplitude of the torque ripple is slightly higher. As shown above KF works properly and proves the robustness of the proposed speed observer. We can see the insensibility of the control algorithm at free acceleration test.

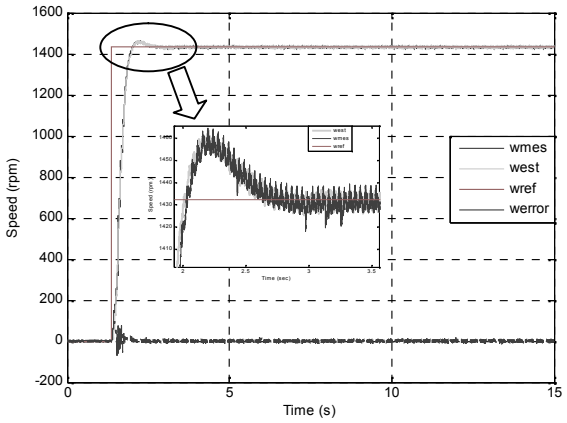

Fig. 3. The reference, actual, estimated and error estimated speed at no load condition.

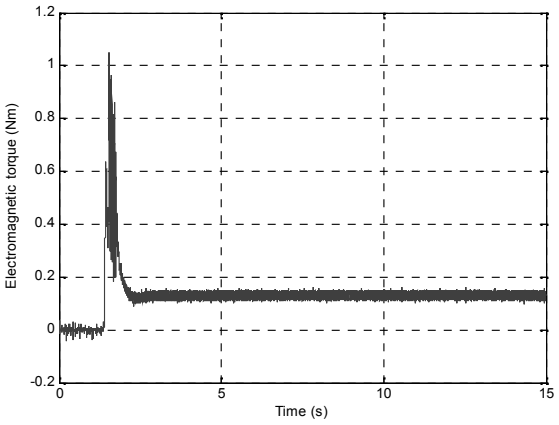

a)

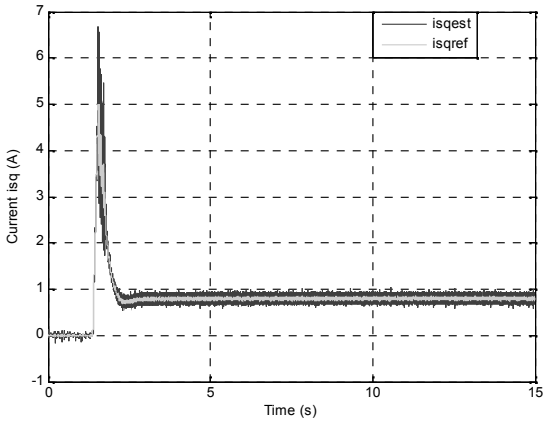

b)

Fig. 4. a) Response electromagnetic torque, b) estimated stator currents evolution (no load condition).

Figure 5 shows the speed-sensorless control performance where the load was applied and omitted. The estimated speed coincides exactly with the real speed even the load torque application instant. It is seen that there is only a very small speed estimation error during the speed transient. From these results, it is

shown that the proposed speed-sensorless control algorithm has good performances both during large signal transient operation.

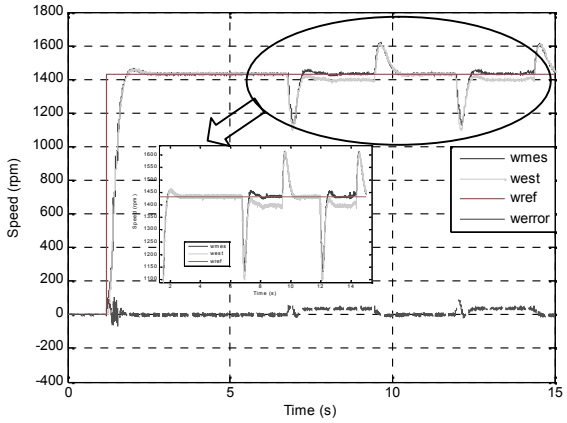

Fig. 5. The reference, actual, estimated and error estimated speed at speed applied a load at 5-7-13-15 sec.

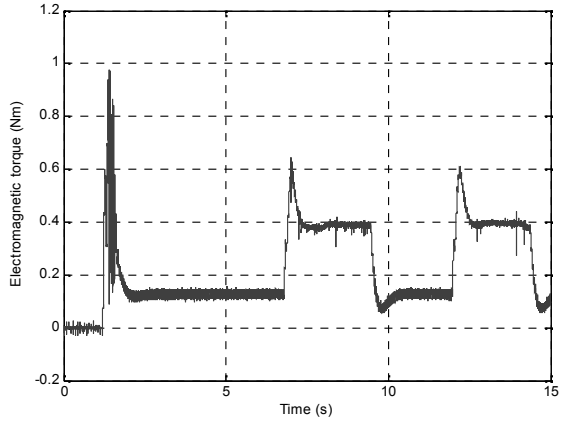

a)

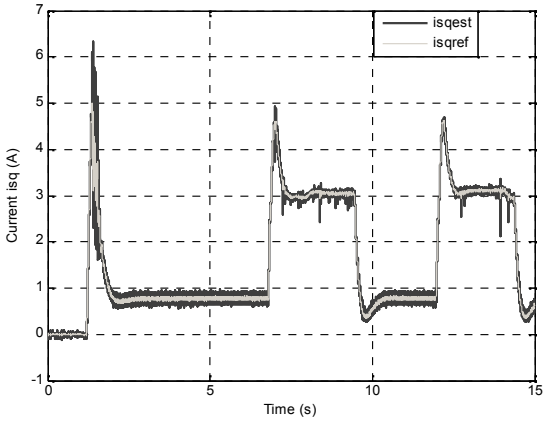

b)

Fig. 6. a) Response electromagnetic torque, b) estimated stator currents evolution (with load applied).

The real and estimated stator currents and the estimated electromagnetic torque, when the motor is running at high speed with load applied, are given by fig. 6a and b. these figures show that the real and the estimated stator currents, the estimates electromagnetic torque are in close agreement.

Figure 7 shows the behavior the motor at nominal speeds under variable load conditions.

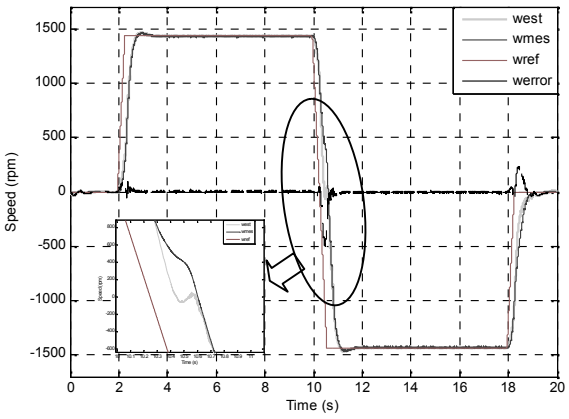

Fig. 7. The reference, actual, estimated and error estimated speed at speed reversal with no load condition.

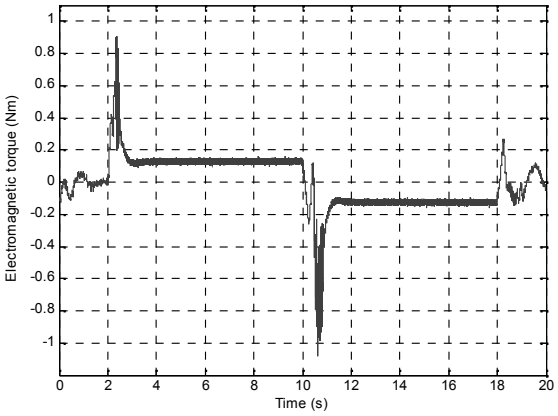

a)

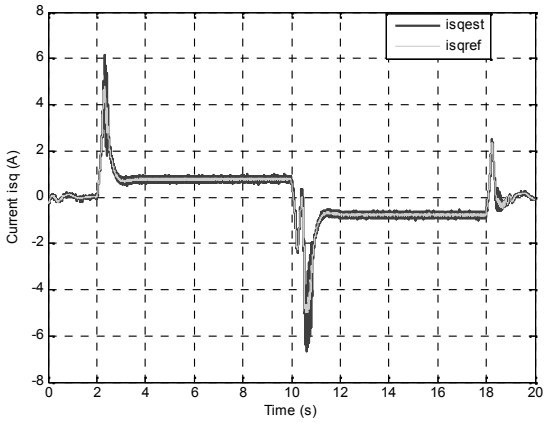

b)

Fig. 8. a) Response electromagnetic torque, b) estimated stator currents evolution. (reversal speed with no load).

The reference speed is set to 1490 rpm at t=2 sec. Then the set point is changed to -1490 rpm at t=10 sec without any load. It is clear that the speed response exhibits good performances at both dynamics regimes. The result clearly shows that the estimated speed

follows the actual speed and the error is not significant.

The results shown in fig. 8a-b illustrate, the electromagnetic torque, actual and estimated stator currents trajectory. These results made the drive remain stable and this condition can be maintained indefinitely

The second experiment, the controller was tested under with the speed dependent load produced by the synchronous machine.

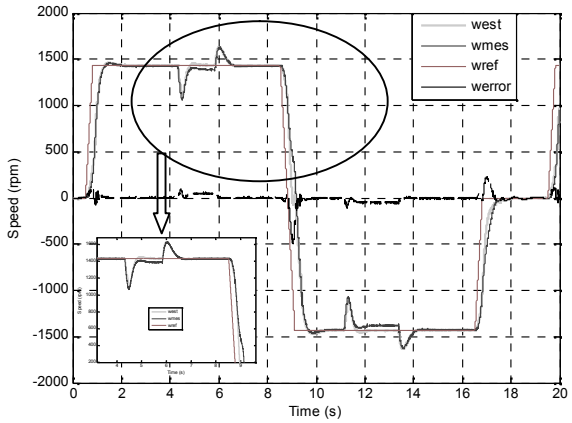

Fig. 9. The reference, actual, estimated and error estimated speed at speed applied a load at 5-7-13-15 sec.

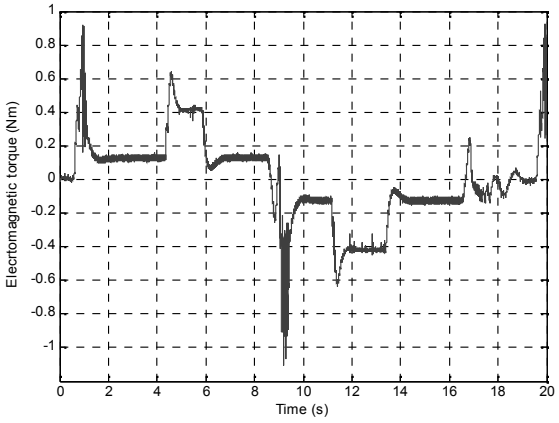

a)

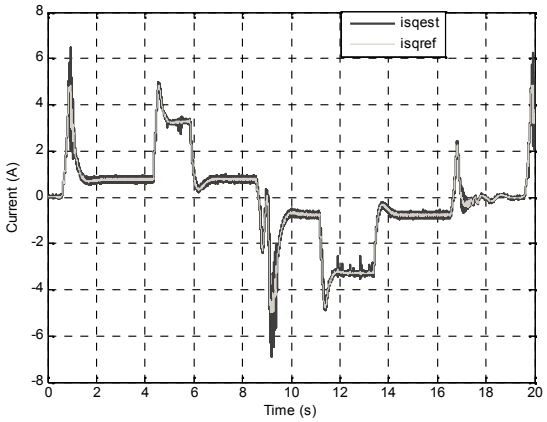

b)

Fig. 10. a) Response electromagnetic torque, b) estimated stator currents evolution. (reversal speed, load applied).

The reversal speed response of the motor is shown in fig 7 at high speeds without load and in figure 9 under different levels of load torque. From inspection of fig.10a-b, it is possible to verify the excellent behavior of the proposed algorithm. In fact, the error on the estimation both of the stator currents and of the electromagnetic torque are always very small (<2%, by referring to the actual values)

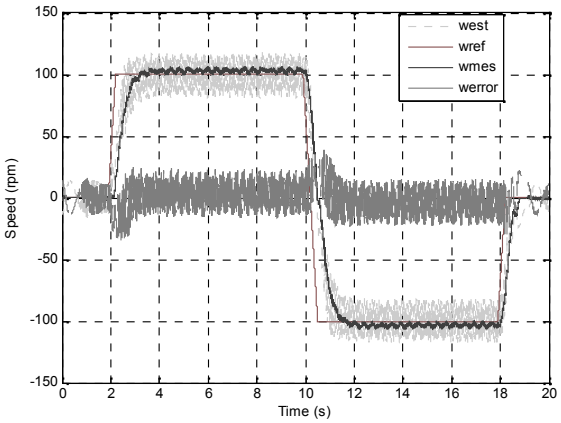

Fig. 11. The reference, actual, estimated and error estimated speed at speed applied at low and reversal speed

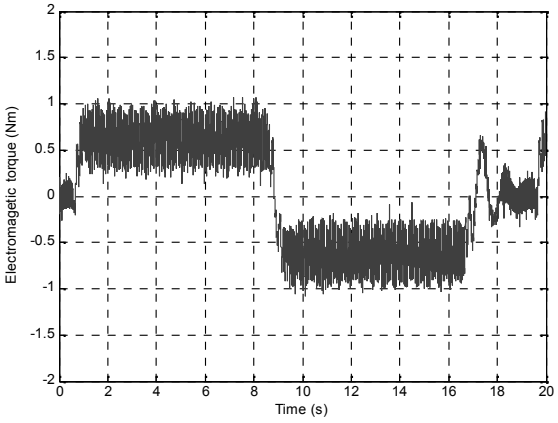

a)

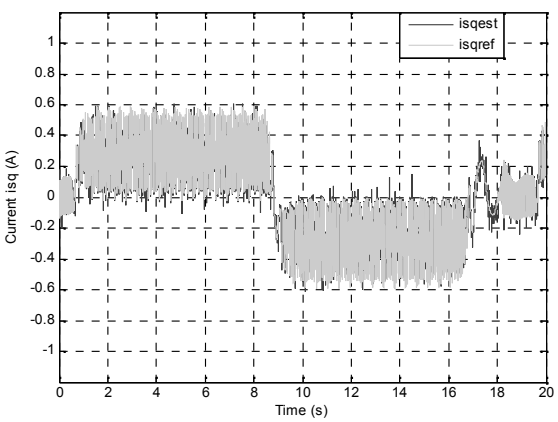

b)

Fig. 12. a) Response electromagnetic torque, b) estimated stator currents evolution (at low speed with reversal)

To test the performance of the sensorless drive at low speed without load. The drive is subjected to speed step down from 100 rpm to -100 rpm (see fig 11).

We can see that the speed follow perfectly the speed reference. However, it is important to note that the control system demonstrates a good performance even under those variations. We note that the performance degrades as approaching the low speed region and fails to provide large oscillations.

Figure 12a and b show torque and stator current estimation in the low speed operation.

Excellent tracking performance was obtained no study state error and no overshoot and control performance of the drive is acceptable for load disturbance. The gotten results show the effectiveness of the proposed control scheme.

8. Conclusion

Both observers presented in the paper can estimate the speed in an electrical drive system. The values of the speed estimated on-line can be used by the control of the electrical drive systems in speed range. The main features are the following:

- The rotor speed of the motor is estimated by reference model with Kalman filter observers.
- To obtain a high-dynamic current sensorless control, a current to voltage feed forward decoupling and a good dynamic correction are obtained.
- Moreover, an accurate dynamic limitation of the real electromagnetic torque is obtained.
- The final algorithm can be implemented with relatively few instructions with execution times of each algorithm 167 μs .
- Results of the dynamic and steady state behavior of a sensorless speed control of an induction motor are given.
- The results were satisfactory.
- Both at low, at load applied, at high and reversal motor speed the proposed control scheme is working very well and proves a robustness of the proposed control structure in dSPACE environment.
- The described control system is a solution without mechanical sensors for a wide range of applications where good steady state and dynamic properties are required.

At present, sensor-based controls are still widely used in industrial and transportation applications. But in the near future, speed sensorless-based drive systems will become a practical reality and will be used in many industrial applications. Sensorless-based systems will provide higher reliability and operation in adverse environmental conditions at a lower cost.

Appendix

Table 1
Induction motor parameters

Components	Rating values
Stator resistance	Rs=*11.8*Ω
Rotor resistance	Rr=*11.3085*Ω
Stator/rotor inductance	Ls=Lr=*0.5568*H
Mutual inductance	L_m=*0.6585*H
Moment of inertia	J=*0.0020* Kg.m^2
Viscous friction	*f=3.1165e-004*N.m/rad/sec
Number of pole pairs	p=*2*

References

1. Magurean, R.U, Ilas, C, Bostan, V, Cuibus, M, Radut, V.: *Luenberger, Kalman, neural observers and fuzzy controllers for speed induction motor*. In: Buletinul Institutului Politehnic Iasi Tomul XLVI (L), FASC. 5, 2000.
2. Vas, P.: *Sensorless Vector and Direct torque control.* In: Oxford University Press, New York, 1998.
3. Kwon, W, Won Jin, D.: *A novel MRAS based speed sensorless control of induction motor*. In: proceeding of the 25 Annual conf. of the IEEE Industrial Electronics Society, IECON'99, vol. 2, pp.933-938.
4. Gadoue, S.: *Low speed operation improvement of MRAS sensorless vector control induction motor drive using neural network flux observers*. In: School of Electrical Electronic and Computer Engineering, University of Newcastle upon Tyne, Newcastle upon Tyne, NE1 7RU, UK.
5. K.Shi, L.: *SPEED estimation of an induction motor drive using extended kalman filter*. In: Department of Electrical Engineering, The Hong Kong Polytechnic University,Hung Hom, Kowloon, Hong Kong.
6. Henneberger, G, B.J. Brunsbach, B.J, Klepsch,T.: *Filed-oriented Control of Synchronous and Asynchronous Drives without Mechanical Sensors using a Kalman Filter*. In: Sen AC Motor Drives, IEEE Press, 1996, pp.207-214.
7. Kafallah, M, El Afia, A, Cherifi, A, El Mariami, F, Saad, A, El Moussaoui, B.: *EKF based Speed Sensorless Vector Control of an lnduction Machine.* In: IEEE International Conference on Industrial Technology, (ICIT), 2004.
8. Gimenez, R.B.: *High performance Sensorless vector control of induction motor drives*. In: Thesis Submitted to the University of Nottingham for the degree of Doctor of philosophy, December 1995.
9. Holtz, J, Quan, J.: *Drift and parameter compensated flux estimator for persistent zero stator frequency operation of sensorless controlled induction motors*. In: IEEE Trans. Industry Applications, vol. 39, no. 4, July/August 2003, pp.1052-1060.